JOC The Journal of Organic Chemistry

Article

pubs.acs.org/joc

2′-*O*-[(4-CF_3-triazol-1-yl)methyl] Uridine – A Sensitive ^{19}F NMR Sensor for the Detection of RNA Secondary Structures

Lotta Granqvist and Pasi Virta*

Department of Chemistry, University of Turku, Turku 20014, Finland

Supporting Information

ABSTRACT: A sensitive uridine-derived sensor (viz., 2′-*O*-[(4-CF_3-triazol-1-yl)methyl]uridine, **1**) for ^{19}F NMR spectroscopic monitoring of RNA secondary structures is described. The applicability of **1** is demonstrated by monitoring the thermal denaturation of the following double and triple helical RNA models: (1) a miR 215 hairpin, (2) a poly U−A*U triple helix RNA (bearing two C−G*C^{H+} interrupts), and (3) a polyadenylated nuclear−nuclear retention element complex. In these RNA models, the ^{19}F NMR shift of the 2′-*O*-(CF_3-triazolylmethyl) group shows high sensitivity to secondary structural arrangements. Moreover, **1** favors the desired *N*-conformation, and its effect on both RNA duplex and triplex stabilities is marginal.

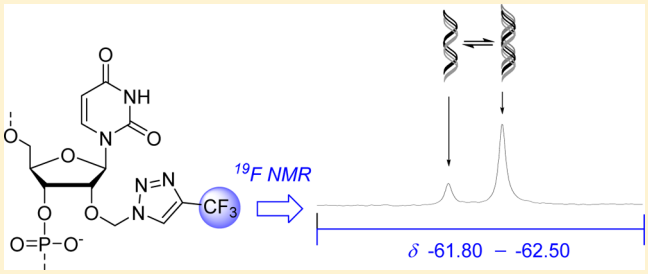

INTRODUCTION

^{19}F NMR spectroscopy has received considerable attention as a method for investigating the structure, dynamics and molecular interactions in oligonucleotides.[1−21] Compared to conventional spectrophotometric methods (UV-, circular dichroism (CD)- and fluorescence-based), the sensitivity is low, and the required ^{19}F-labeling itself is a limitation, yet the superiority of ^{19}F NMR may become distinct with more detailed information about the structure (especially in the local environment) and molar ratios of secondary structural species. The characteristic shift of the ^{19}F nucleus, with wide chemical shift dispersion, is highly sensitive to local van der Waals interactions and electrostatic fields, which facilitates the detection of even minor secondary structural arrangements.[22−26] It may also be worth noting that remarkable breakthroughs have been made in NMR of hyperpolarized fluorine (HPF NMR, several thousand fold enhanced sensitivity) in studies of protein−ligand interactions.[27] There is a likelihood that HPF NMR may soon find applications in oligonucleotides as well.[28]

We and other research groups have focused on developing novel fluorine-labeled nucleoside derivatives, aimed at increasing the sensitivity and straightforwardness of ^{19}F NMR detection of oligonucleotides.[7,16,19,21] The incorporation of a trifluoromethyl group via an appropriate proton coupling barrier into nucleosides is an obvious consequence in this design. The effect of the sensor on the native oligonucleotide structure should additionally be as marginal as possible, while the resulting ^{19}F signal shift should readily reflect secondary structural changes. ^{19}F NMR spectroscopic detection at micromolar oligonucleotide concentration may then be carried out rapidly and reliably by routine instrumentations without the need of ^{1}H decoupling. Micura et al. have recently successfully used 2′-trifluoromethylthio-modified ribonucleic acids as sensors for the ^{19}F NMR spectroscopic detection of RNA−protein and RNA−small molecule interactions and of molar fractions of bistable RNAs.[16,21] While the shift of the 2′-trifluoromethylthio group was highly sensitive to secondary structural changes, unfortunately, this modification markedly decreased the RNA duplex stability. This decrease was a result of strong C-2′-endo (*S*-conformation) preference of these ribonucleosides. We recently used 4-*C*-[(4-trifluoromethyl-1*H*-1,2,3-triazol-1-yl)methyl]thymidine (**2**) as a sensor for monitoring both DNA and RNA secondary structures.[20] This deoxynucleoside, with predominant *S*-conformation, seemingly favored the DNA environment, but it did not decrease the RNA duplex stability either. The equilibrium between the C-2′- and C-3′-endo puckering of **2** was probably facile enough to adopt proper conformation for both types of helices (A and B). Although detailed ^{19}F NMR spectroscopic information by **2** may be gained, the C-4′-position for the label is not the best possible for RNA. The C-4′ site orients the label outward from the RNA helix, which may lead to a modest shift discrimination between the duplex and the single strand. Furthermore, this modification at C-4′ may hardly be expanded to purine nucleosides.

In the present study, we describe a new and promising ^{19}F NMR sensor for RNA, namely, 2′-*O*-[(4-trifluoromethyl-1*H*-1,2,3-triazol-1-yl)methyl]uridine (**1**). The 2′-*O*-(CF_3-triazolylmethyl) group offered a quasi-isolated ^{19}F spin system (as in **2**), and its ^{19}F resonance shift was highly sensitive to secondary structural changes. As expected, this modified nucleoside preferred C-3′-endo sugar puckering (*N*-conformation), and it neither affected the RNA duplex nor the RNA triplex

Received: April 30, 2015
Published: July 27, 2015

DOI: 10.1021/acs.joc.5b00973
J. Org. Chem. 2015, 80, 7961−7970

Scheme 1[a]

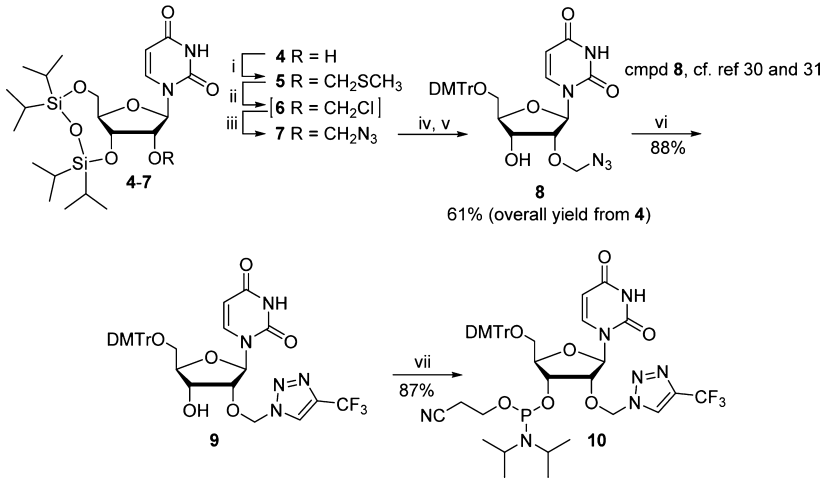

[a](i) DMSO, Ac_2O, AcOH; (ii) SO_2Cl_2, DCM; (iii) NaN_3, DMF; (iv) TBAF, THF; (v) DMTrCl, Py; (vi) 3,3,3-trifluoroprop-1-yne, $CuSO_4$, sodium ascorbate, H_2O, dioxane; (vii) 2-cyanoethyl *N*,*N*-diisopropylphosphoramidochloridite, Et_3N, DCM.

stabilities (demonstrated by UV- and CD-melting profiles of the RNA models studied). Additionally, synthesis of the phosphoramidite derivate (**10**) was simple (Scheme 1), and its incorporation into RNA strands by an automated synthesizer was efficient. The ^{19}F NMR spectroscopic monitoring of thermal denaturation of RNA hairpins (^{19}F-labeled models of miR 215[29] and polyadenylated nuclear (PAN)) and RNA triple helices (^{19}F-labeled models of a poly U−A*U model, interrupted by two C−G*C^{H+} triplets and a polyadenylated nuclear−nuclear retention element (PAN-ENE) complex) was demonstrated. For the monitoring of thermal denaturation of an RNA hairpin (miR 215 model), the shift response of **1** was compared to those of two other potential sensors (**2** and 4′-*C*-(4-trifluorophenyl)uridine (**3**), the latter also synthesized in the present study). Figure 1 shows the structures of sensors **1**−**3**.

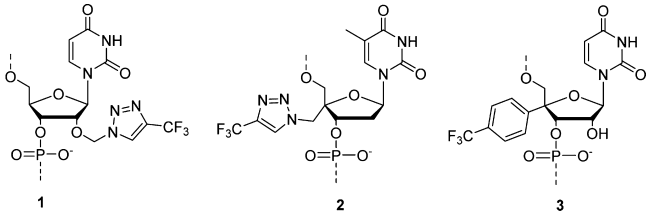

Figure 1. Structures of the ^{19}F NMR sensors (**1**−**3**) studied.

RESULTS AND DISCUSSION

Synthesis of the Phosphoramidite Building Blocks of 2′-*O*-[(4-Trifluoromethyl-1*H*-triazol-1-yl)methyl]uridine (10) and 4′-*C*-(4-Trifluorophenyl)uridine (20). 2′-*O*-(Azidomethyl)ribonucleosides may be prepared from the corresponding 2′-*O*-(methylthiomethyl)-3′,5′-*O*-(1,1,3,3-tetraisopropyl-1,3-disiloxanediyl) ribonucleosides.[30,31] 2′-*O*-(Azidomethyl)-5′-*O*-(4,4′-dimethoxytrityl)uridine (**8** in Scheme 1) was obtained following this reported protocol and treated with gaseous 3,3,3-trifluoroprop-1-yne in the presence of $CuSO_4$ and sodium ascorbate to yield 2′-*O*-[(4-trifluoromethyl-1*H*-1,2,3-triazol-1-yl)methyl]uridine (**9**) in 88% yield. It may be worth noting that 3,3,3-trifluoropropyne is able to react with alkylazides also in copper-free conditions, but a mixture of 4- and 5-trifluoromethyl-1*H*-1,2,3-triazoles may be obtained.[32] Phosphitylation of the 3′-OH group gave the desired phosphoramidite **10**. As seen, the synthesis of the phosphoramidite derivative of **1** was rather straightforward (six synthetic steps from commercially available **4**, with an overall yield of 47%).

Synthesis of the phosphoramidite **20** is outlined in Scheme 2. Ketone **11** could be prepared in a gram scale according to the literature.[33] Stereoselective Grignard reaction with 4-bromobenzotrifluoride to **11** gave the desired addition product **12** in 73% yield (2*R*/2*S*, 7:1, *n*/*n*). The TBDMS group (**12**) was then replaced by the benzoyl group (**13**), since the premature exposing of the 5-OH group may lead to an undesired pyranose formation (cf. the forthcoming synthetic steps between **13**, **14**, and **15**). Oxidative release of the anomeric center (**14**), acid-catalyzed removal of the isopropylidene group, perbenzoylation (**15**), and N-glycosidation gave 4′-*C*-[4-(trifluoromethyl)-phenyl]uridine (**16**) in 38% overall isolated yield from **11**. The neighboring group participation via the 2′-*O*-benzoyl group gave predominantly β-N-glycosidated product (1′*R*). A clear 2D NOESY correlation between $H^{1'}$ and aromatic protons of CF_3Ph may be observed, which further verified the desired 4′*R*-configuration (see the Supporting Information). 4,4′-Dimethoxytritylation of **17** was the bottleneck of the synthesis (**18** in 40% yield). Because of the steric hindrance of the CF_3Ph group, the reactivity of the 5′-OH group was close to that of the 2′-OH group, and a remarkable amount of 2′,5′-bistritylated uridine was obtained. Several trials were conducted to overcome this problem. As an example, selective benzoyl removal from the primary hydroxyl group of **16** using $[t$BuSnOHCl$]_2$ in methanol[34] followed by 4,4′-dimethoxytritylation and subsequent NaOMe-catalyzed removal of 2′-*O*- and 3′-*O*-acetyl groups gave **18** in 51% yield. In spite of the slight improvement of yield, this method was somewhat complex, and repeating of the reaction from **17** to **18** (**17** readily recovered from the bistritylated uridine) turned out to be practically the best route for **18**. The 2′-OH could be selectively silylated by a TOM group (**19**), and phosphitylation of the 3′-OH (**27**) group gave finally **20**. The overall yield from **11** to **20** remained as low as 6%.

DOI: 10.1021/acs.joc.5b00973
J. Org. Chem. 2015, 80, 7961−7970

Scheme 2[a]

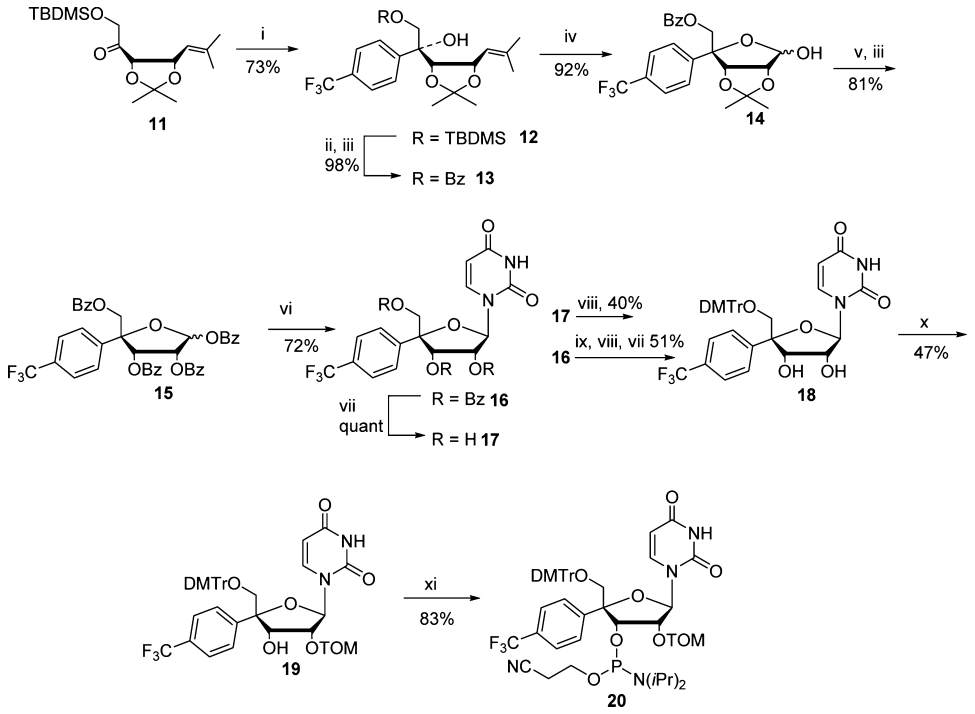

[a](i) 4-Bromobenzotrifluoride, Mg, Et_2O; (ii) TBAF, THF; (iii) BzCl, DMAP, Py; (iv) 1: OsO_4, 4-methylmorpholine *N*-oxide, acetone; 2: H_5IO_6, THF; (v) HCl, H_2O, dioxane; (vi) TMSOTf, 2,4-bis(trimethylsilyloxy)uridine, MeCN; (vii) NaOMe, MeOH; (viii) DMTrCl, Py; (ix) [*t*BuSnOHCl]$_2$, MeOH; (x) DIEA, Bu_2SnCl_2, triisopropylsilyloxymethyl chloride, 1,2-dichloroethane; (xi) 2-cyanoethyl *N*,*N*-diisopropylphosphoramidochloridite, Et_3N, DCM.

Stability of 2′-*O*-[(4-Trifluoromethyl-1*H*-1,2,3-triazol-1-yl)methyl]uridine and 4′-*C*-(4-Trifluorophenyl)uridine in Acidic and Basic Conditions. 2′-*O*-[(4-Trifluoromethyl-1*H*-1,2,3-triazol-1-yl)methyl]uridine and 4′-*C*-(4-trifluorophenyl)uridine may in principle undergo acid-catalyzed hydrolysis of the 2′-*O*-methyltriazolyl group (**1**) and epimerization at the C-4′-position/ring opening of the ribose sugar (**3**), respectively. The stability of these nucleosides has been evaluated in 80% aqueous acetic acid at 25 °C and additionally in concentrated aqueous ammonia at 55 °C. Both nucleosides seemed virtually intact in these treatments after 3 days. Potential side reactions within the nucleoside units (**1** and **3**) are therefore hardly expected, for example, in the treatments required for the automated RNA synthesis (i.e., removal of DMTr and nucleobase protections) or in the prolonged incubation at elevated temperature required for the ^{19}F NMR melting temperature studies of the synthesized RNAs.

Sugar Conformation of the Sensors. An optimized Karplus relation[35] for ^{1}H NMR H1′−H2′ coupling constants ($J_{H1'-H2'}$) was used to evaluate the sugar puckering of the sensors (as nucleosides). Assuming a pure *N*/*S* (C3′/C2′-endo) equilibrium, 2′-*O*-(4-CF_3-triazolylmethyl)uridine (cf. **1**) existed predominantly as a C3′-endo conformation (*N* 67%, $J_{H1'-H2'}$ = 3.3 Hz). The corresponding values for 4′-C-(4-CF_3-triazolylmethyl)thymidine (cf. **2**), 4′-C-(4-trifluoromethylphenyl)uridine (cf. **3**), and uridine were *S* 72% ($J_{H1'-H2'}$ = 7.3 Hz), *N* 48% ($J_{H1'-H2'}$ = 5.3 Hz), and *N* 53% ($J_{H1'-H2'}$ = 4.8 Hz), respectively. While the duplex formation usually increases the favored C3′-endo population of a single RNA residue (in an A-form RNA double helix),[21] relatively high C2′-endo populations for single-stranded residues may however be observed.[16,21] Short RNA sequences (5′-AU**1**A-3′ and 5′-AUUA-3′) were additionally prepared, and the *N*/*S* ratio for each residue was determined. The C3′-endo population of **1** in the AU**1**A sequence was now *N* 32% ($J_{H1'-H2'}$ = 6.9 Hz), and the corresponding values (*N* %) for other single-stranded residues were as follows: 48% ($J_{H1'-H2'}$ = 5.3 Hz, A), 50% ($J_{H1'-H2'}$ = 5.1 Hz, A), and 46% ($J_{H1'-H2'}$ = 5.5 Hz, U). In the AUUA model, the corresponding values (*N* %) were 50% ($J_{H1'-H2'}$ = 5.1 Hz, A), 46% ($J_{H1'-H2'}$ = 5.5 Hz, A), 44% ($J_{H1'-H2'}$ = 5.7 Hz, U), and 46% ($J_{H1'-H2'}$ = 5.5 Hz, U).

Oligonucleotide Synthesis. Fluorine-labeled oligoribonucleotides (**ORN 1**−**5**, see structures in Table 1 and Figures 3−5) were synthesized on a 1.0 μmol scale using an automatic DNA/RNA synthesizer. Benzylhiotetrazole was used as an activator, and coupling times of 300 s for the standard RNA building blocks and of 600 s for the fluorine-labeled nucleosides (**10** and phosphoramidite derivative of **2**) were used. The coupling efficiency of **10** and the phosphoramidite derivative of **2** in the automatic synthesizer did not differ from those of the standard 2′-*O*-TBDMS-protected RNA building blocks. However, a manual coupling (see the Experimental Section) with a higher (0.11 mol L^{-1}) phosphoramidite concentration was required to give an acceptable coupling yield (90% according to a DMTr assay) for **20**. The oligoribonucleotides were released from the support with a mixture of concentrated ammonia and ethanol (3:1, v/v, 3 h at 55 °C and overnight at rt). The silyl protections were removed by a treatment with triethylamine trihydrofluoride followed by RP cartridge filtration. The filtrates were purified by reverse-phase high-performance liquid chromatography (RP-HPLC), and the authenticity of **ORN 1**−**5** was verified by electrospray ionization time-of-flight mass spectrometry ESI-TOF MS (Table 1). A representative example (**ORN 4**) of the RP-HPLC profiles of crude ORNs

DOI: 10.1021/acs.joc.5b00973
J. Org. Chem. 2015, 80, 7961−7970

Table 1. Observed and Calculated Molecular Masses of ORN 1−5

ORN 1-3: 5'-**CA**C AGG AAA AUG ACU UCG GCC AAU A***U***U CUG **UG**-3'

ORN 4: 5'-AAA GAA AAG A~ UCU U***U***U CUU U~ UUU CUU UUC-3'

ORN 5: 5'-**GGC U**GG GUU UUU CC***U*** UCG AAA GAA GGU UUU UAU CCC **AGU C**-3'

ORN 1, **ORN 4** and **ORN 5**: ***U*** = **1**
ORN 2: ***U*** = **2**
ORN 3: ***U*** = **3**
bold letters are 2'-*O*-methyl ribonucleotides

~ = 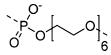

entry	^{19}F-labeled RNA	isolated yield	observed molecular mass	calculated average molecular mass
1	**ORN 1**	7%	10 438.9[a]	10 437.4
2	**ORN 2**	10%	10 435.2[a]	10 435.4
3	**ORN 3**	5%	10 431.9[a]	10 432.4
4	**ORN 4**	7%	10 219.4[a]	10 219.2
5	**ORN 5**	7%	12 989.4[b]	12 989.9

[a]Calculated from the most intensive isotope combination at $[(M - 10H)/10]^{-10}$. [b]Calculated from the most intensive isotope combination at $[(M - 13H)/13]^{-13}$.

and of MS spectra are shown in Figure 2. Isolated yields **ORN 1−5** ranged from 5% to 10% (Table 1).

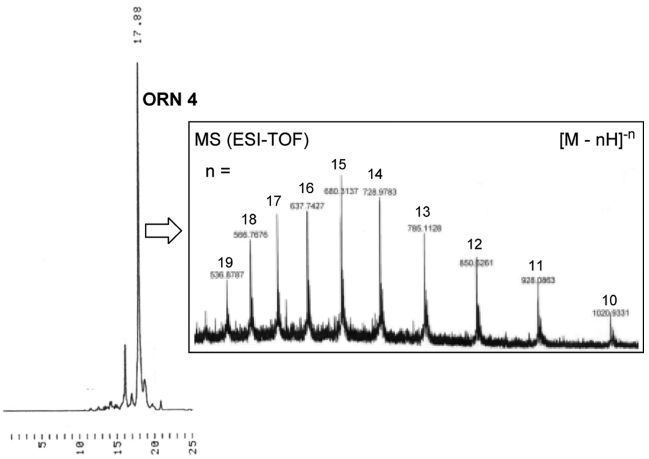

Figure 2. Example (**ORN 4**) of RP-HPLC profiles of the crude product mixtures and of ESI-TOF MS spectra of the homogenized products.

Melting Temperature Studies of Fluorine-Labeled RNAs. UV-melting temperatures of the ^{19}F-labeled oligoribonucleotides **ORN 1−4** and the **ORN 5** + A_9 complex and the ΔT_m values in comparison to those obtained with unmodified oligoribonucleotides (***U*** = **1** or uridine, cf. structures in Figures 3−5) are shown in Table 2 (2 μmol L^{-1} of each ORN in a mixture of 0.1 mol L^{-1} NaCl and 10 mmol L^{-1} sodium cacodylate at pH 7.0). As seen, none of the studied sensors (**1−3**) affected the hairpin stability. The effect of **1** on the stability of the triple helical structure of **ORN 4** was also marginal (UV-melting profiles of **ORN 1−3** are shown in Figure 3, and those of **ORN 4** and the **ORN 5** + A_9 complex are shown in the Supporting Information).

^{19}F NMR Measurements. From the ^{19}F NMR spectroscopic point of view, the minimal requirement for the sensor is the ^{19}F NMR shift, which responds well to hybridization. As a matter of fact, this shift discrimination (between the double helix and single strand) alone may be expanded for many more interesting ^{19}F NMR applications (cf. characterization of an RNA invasion[9,12,20] and determination of molar fractions of bistable RNAs[3,16]). As a first ^{19}F NMR experiment, **1−3** were incorporated at the same site of a miR 215 hairpin model (**ORN 1**, **ORN 2**, and **ORN 3**, ***U*** = **1**, **2**, and **3**, respectively), and their ^{19}F NMR applicability to detect thermal denaturation of this hairpin RNA was evaluated. The ^{19}F NMR measurements were carried out using a RNA concentration of 50 μmol L^{-1} (**ORN 1−3** in a mixture of 0.1 mol L^{-1} NaCl and 10 mmol L^{-1} sodium cacodylate at pH 6.0). The ^{19}F NMR shift versus temperature profiles between 30 and 70 °C are shown in Figure 3a, and the profiles of the shift differences versus temperature after subtraction of a passive temperature-dependent shift (0.014 ppm K^{-1}) are shown in Figure 3b. Each sensor gave coalescence signal, which discriminated between the miR 215 hairpin (**A**) and the denaturated form (**B**). The signals referring to the hairpin (**A**) shifted to lower magnetic field and negative S-curves were obtained in each case. The inflection points showed nearly the same $T_m^{A/B}$ value (ca. 55 °C), but **1** gave the largest shift dispersion (Figure 3b: $\Delta\delta$: **1**: 0.82 ppm; **2**: 0.23 ppm; and **3**: 0.12 ppm between 30 and 70 °C). The 4′-C-fluorine labels (**2** and **3**) were probably relatively naked at this site (***U***) in the stem region (i.e., the modest change in the local environment around C-4′ of **2** and **3** upon hybridization led to a small shift response.). The large downfield shift of **1** was most likely related to the shielding of H-5′,5″ protons of the preceding nucleotide in the helix. Because of the smallest shift dispersion obtained by **3** (together with the complex synthesis of **20** and the reduced coupling efficiency in the automated RNA synthesis), further effort to prove the potential of this seemingly promising sensor (**3** bears free 2′-OH unlike **1** and **2**) was excluded. Sensor **2** was in turn primarily designed for the DNA environment, and its applicability has previously been described.[20] The superiority of **1** (the large shift dispersion, the simple synthesis of **10**, and its efficient coupling) among these three sensors (**1−3**) seemed obvious, and its functionality was then further evaluated.

The ^{19}F NMR spectra obtained upon denaturation of **ORN 1** are shown in Figure 3c. In addition to the main coalescence signal, there may be seen a minor signal (marked with an asterisk). The shift of the minor signal followed mainly the passive temperature-dependent shift (slope: 0.014 ppm °C^{-1}), but a modest downfield turn was observed on approaching the denaturation temperature ($T_m^{A/B}$ = 55 °C). The downfield turn and the continuously reduced molar fraction in decreasing temperature refer to an incomplete coalescence signal (i.e., * refers to **B**), but the minor signal may also partly be traced to hydrolytic cleavage products. Partial hydrolytic cleavage of **ORN 1** (and increase of the minor signal *) was observed after prolonged incubations at elevated temperatures.

The scope of **1** was then expanded for ^{19}F NMR spectroscopic monitoring of RNA triple helix/duplex/single-strand conversion. Sensor **1** was incorporated to a previously studied poly U−A*U model (interrupted by two C−G*C^{H+} triplets; note: two pyrimidine strands and one purine strand are connected to each other by hexaethylene glycol spacers, **ORN 4**, Figure 4).[36] The triplex/duplex/single-strand conversion was monitored by ^{19}F NMR spectroscopy using 50 μmol L^{-1} **ORN 4** in a mixture of 0.1 mol L^{-1} NaCl and 10 mmol L^{-1} sodium cacodylate at pH 7.0. Like above with the miR 215 model, a well-behaving coalescence signal was obtained for the melting of the intramolecular double helix (Figure 4a: **D** vs **E**). The ^{19}F

DOI: 10.1021/acs.joc.5b00973
J. Org. Chem. 2015, 80, 7961−7970

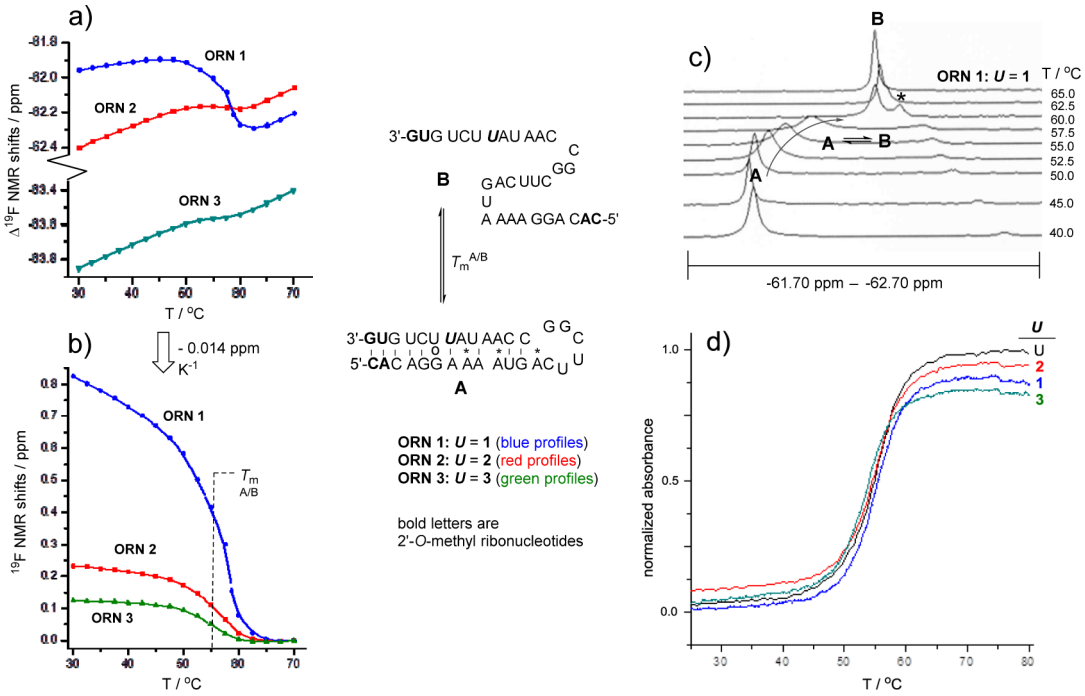

Figure 3. (a, b) ^{19}F NMR shift vs temperature profiles obtained by sensors **1**–**3** upon thermal denaturation of a miR 215 hairpin model (**A**/**B**); (c) ^{19}F NMR spectra of **ORN 1** in different temperatures (50 μmol L^{-1} of **ORN 1** in 0.1 mol L^{-1} NaCl and 10 mmol L^{-1} sodium cacodylate at pH 6.0); (d) corresponding UV-melting profiles of **ORN 1**–**3** (T_m values listed in Table 2).

Table 2. UV-Melting Experiments (T_m/°C) of the ^{19}F-Labelled Oligoribonucleotides (ORN 1–5)

entry	oligoribonucleotide	duplex T_m/°C	triplex T_m/°C
1	**ORN 1**	52.9 (−0.7)	–
2	**ORN 2**	53.1 (−0.5)	–
3	**ORN 3**	53.4 (−0.2)	–
4	**ORN 4**	59.3 (−0.6)	21.8 (−1.6)
5	**ORN 4**[b]	60.4 (−0.6)[b]	26.5 (+0.1)[b]
6	**ORN 5**	68.8 (−0.2)	–
7	**ORN 5** + A_9	68.3 (−0.8)	n.d.[a]

[a]n.d.: absorbance change referring to denaturation of **ORN 5** + A_9 complex severely overlapped with background absorbance of **ORN 5**. Inflection point cannot be determined (profiles in the Supporting Information). ΔT_m (in parentheses) in comparison to those obtained with unmodified oligoribonucleotides (*U* = uridine). Conditions: 10 mmol L^{-1} sodium cacodylate (pH = 7.0), 0.1 mol L^{-1} NaCl, 2.0 μmol L^{-1} of each oligonucleotide, UV detection at 260 nm. [b]1.0 equiv of neomycin was added to a mixture.

NMR shift versus temperature profile as a negative S-curve is shown in Figure 4b, in which the inflection point shows $T_m^{D/E}$ = 59 °C, a value between the double helix (**D**) and the single strand (**E**). At a lower temperature (40 °C), a separate new ^{19}F NMR resonance signal appeared. When the temperature was decreased further, a relative peak area of this new signal increased, and it was equal sized with the duplex signal at 32.5 °C (Figure 4a). This new signal refers to a triplex, which denaturates at 32.5 °C. In turn, separate signals for the duplex and triplex indicate equilibrium of an intermolecular process (i.e., **C**). The ^{19}F NMR measurements were then additionally carried out at a lower **ORN 4** concentration. As seen in Figure 4a, the triplex formation was concentration-dependent: In the mixture of 50 μmol L^{-1} **ORN 4**, the duplex and triplex signals were equal sized at 32.5 °C (= $T_m^{C/D}$), whereas in the mixture of 5 μmol L^{-1} **ORN 4**, only a trace of the triplex signal may be seen. Thus, the observed signal refers to a triple helical dimer of **ORN 4** (i.e., **C**) and not to an expected intramolecular triplex (**F**).[36] Molar fractions of **C**, **D**, and **E**, shown in Figure 4c, may be finally extracted from the relative peak areas of the signals (**C** vs **D**, Figure 4a) and from the shift versus temperature profile (**D** vs **E**, Figure 4b) after subtraction of the passive temperature-dependent shift.

The PAN-ENE complex has recently received considerable medical and biological attention.[37,38] PAN RNA is a long noncoding RNA produced by the oncogenic gammaherpesvirus KSHV, it accumulates extraordinary high levels during lytic infection, and it is required for the production of late viral proteins. Triple helix formation with ENE is essential for this high accumulation. Although spectrophotometric data of this complex have been documented, the inflection point of the denaturation of the PAN-ENE complex is usually severely overlapped by the strong background absorbance of PAN. However, more accurate determination of molar fractions of the secondary structural species throughout the denaturation is required, for example, for the determination of thermodynamic parameters, and therefore, an alternative insight for the monitoring of this complex would be advisible. In the present study, applicability of ^{19}F NMR spectroscopy using **1** as a sensor for the more detailed denaturation analysis of a model of the PAN-ENE complex has been demonstrated. **ORN 5** (Figure 5) was mixed with A_9, and the triplex/duplex/single-strand conversion was monitored by ^{19}F NMR spectroscopy (50 μmol L^{-1} **ORN 5** and A_9 in a mixture of 0.1 mol L^{-1} NaCl and 10 mmol L^{-1} sodium cacodylate at pH 7.0). The bipartite triple helical structure **G** in Figure 5 has previously been described for the same PAN-ENE model system[38] (in our case **1** and four 2′-*O*-methyl ribonucleotides have been incorporated into the structure). As seen in ^{19}F NMR spectra (Figure 5a), the system (**ORN 5** + A_9 in different temperatures) behaved in a similar manner as described above for **ORN 4**. A well-

DOI: 10.1021/acs.joc.5b00973
J. Org. Chem. 2015, 80, 7961–7970

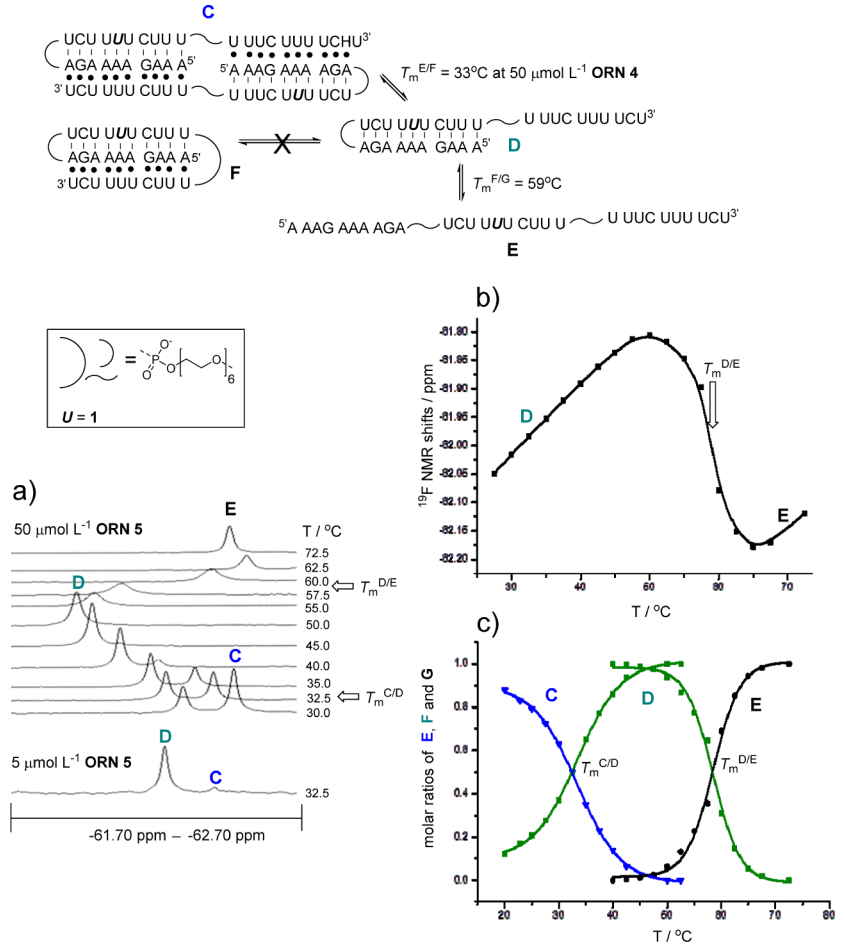

Figure 4. (a) ^{19}F NMR spectra of **ORN 4** in different temperatures (5 and 50 μmol L^{-1} **ORN 4** in 0.1 mol L^{-1} NaCl and 10 mmol L^{-1} sodium cacodylate at pH 7.0); (b) ^{19}F NMR shift versus temperature profile of **ORN 4** (**D** vs **E**); (c) molar fractions of dimeric triple helix **C**, duplex **D**, and single strand **E** of **ORN 4**.

behaving coalescence signal was obtained for the hairpin melting (**H** vs **I**), whereas the intermolecular complex formation (**ORN 5** + A_9) gave a separate signal (**G**). Despite the labeling site that was clearly outside the expected binding region, **1** could distinguish surprisingly well between the bipartite triple helical structure of **ORN 5** + A_9 (**G**) and the **ORN 5** hairpin (**H**). Molar fractions of the secondary structures upon hairpin denaturation (**H** vs **I**) may be extracted from the shift of the coalescence signal after subtraction of the passive temperature-dependent shift, whereas the molar fractions of **G** and **H** may be extracted from the relative peak areas of the ^{19}F NMR resonance signals (Figure 5b). Melting temperatures of $T_m^{G/H}$ = 20 °C and $T_m^{H/I}$ = 68 °C were obtained. The measurements were additionally carried out in the presence of neomycin (5 equiv, a known groove binder for RNA triple helices[39]). A remarkable stabilization of the triple helical complex ($T_m^{G'/H'}$ = 48 °C, ΔT_m = 28 °C) was expectedly observed, but the stability of the hairpin was also affected by neomycin: the melting temperature ($T_m^{H'/I'}$ = 83 °C) of hairpin **H** increased by ΔT_m = 16 °C.

CONCLUSION

2′-*O*-[(4-Trifluoromethyl-1*H*-1,2,3-triazol-1-yl)methyl]uridine (**1**) proved to be an excellent ^{19}F NMR sensor for the characterization of RNA secondary structures. The advantages of **1** may be summarized as follows: (1) synthesis of the corresponding phosphoramidite (**10**) was straightforward; (2) the coupling efficiency of **10** in automated RNA synthesis; (3) the ^{19}F NMR signal of **1** was sensitive to secondary structural changes with relatively wide shift dispersion; and (4) **1** did not affect either the RNA duplex or RNA triplex stabilities (duplex ΔT_m < 1 °C and triplex ΔT_m < 2 °C). The applicability of **1** was demonstrated for the ^{19}F NMR spectroscopic monitoring of thermal denaturation of RNA hairpins (**ORN 1**, **ORN 4**, and **ORN 5**) and triplex/duplex/single-strand conversion upon denaturation of a poly U−A−U model (interrupted by two C−G*C^{H+} triplets, **ORN 4**) and a model of the PAN-ENE complex (**ORN 5** + A_9). The applicability of ^{19}F NMR spectroscopy for the monitoring of an RNA triple helix was described for the first time.

EXPERIMENTAL SECTION

General Remarks. Dichloromethane and MeCN were dried over 3 Å molecular sieves, and triethylamine was dried over CaH_2. The NMR spectra were recorded at 500 MHz. The chemical shifts in the ^{1}H and ^{13}C NMR spectra are given in parts per million (ppm) from the residual signal of the deuterated solvents CD_3OD and CD_3CN. ^{31}P shifts are referenced to external H_3PO_4, and ^{19}F shifts are referenced to external CCl_3F. The mass spectra were recorded using ESI.

*5′-O-(4,4′-Dimethoxytrityl)-2′-O-[(4-trifluoromethyl-1H-1,2,3-triazol-1-yl)methyl]uridine (**9**).* To a mixture of 5′-*O*-(4,4′-dimethoxytrityl)-2′-*O*-azidomethyluridine[30,31] (**8**, 0.33 g, 0.55 mmol) in DMSO (3.5 mL), aqueous solutions of $CuSO_4$ (0.1 mol L^{-1}, 55 μL, 5.5 μmol)

DOI: 10.1021/acs.joc.5b00973
J. Org. Chem. 2015, 80, 7961−7970

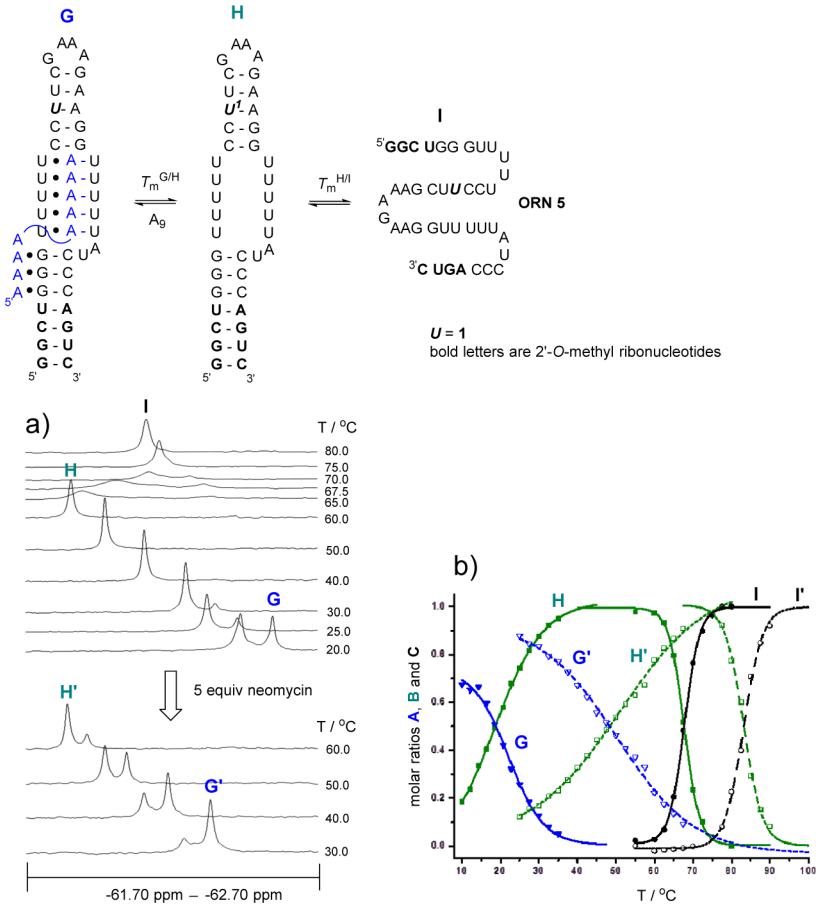

Figure 5. (a) ^{19}F NMR spectra of **ORN 5** + A_9 in different temperatures in the presence and absence of neomycin (5 equiv) (50 μmol L^{-1} **ORN 5** and A_9 in 0.1 mol L^{-1} NaCl and 10 mmol L^{-1} sodium cacodylate at pH 7.0); (b) molar fractions of different secondary structures in different temperatures (symbols **G**, **H**, **I**, and solid lines refer to a mixture without neomycin; symbols **G′**, **H′**, **I′**, and dotted lines to a mixture in the presence of neomycin.

and sodium ascorbate (0.1 mol L^{-1}, 0.55 mL, 55 μmol) were added. The reaction was carried out in a sealed tube, placed in an ice bath, and bubbled with gaseous 3,3,3-trifluoropropyne for 5 min. The reaction mixture was then stirred at room temperature for 2 days, during which time the gas was added seven times in an ice bath along with additions of the aqueous solutions of $CuSO_4$ and sodium ascorbate (the same amounts as above). The reaction mixture was then partitioned between dichloromethane and saturated aqueous $NaHCO_3$. The organic phase was separated, dried over Na_2SO_4, and evaporated to dryness. The residue was purified by silica gel chromatography (0.1% Et_3N, 5% MeOH in DCM) to yield 0.34 g (88%) of the product **9** as a yellowish foam. ^{1}H NMR (500 MHz, $CDCl_3$): δ 8.31 (s, 1H), 8.04 (d, 1H, J = 8.2 Hz), 7.39−7.38 (m, 2H), 7.32−7.23 (m, 7H), 6.87−6.85 (m, 4H), 6.17 (d, 1H, J = 11.1 Hz), 6.04 (d, 1H, J = 11.1 Hz), 5.93 (d, 1H, $J^{1'2'}$ cannot be determined), 5.34 (d, 1H, J = 8.2 Hz), 4.49 (dd, 1H, J = 8.2 and 5.2 Hz), 4.27 (dd, 1H, J = 5.2 Hz and $J^{1',2'}$), 4.11 (m, 1H), 3.81 and 3.80 (2 × s, 2 × 3H), 3.61 (dd, 1H, J = 11.4 and 2.0 Hz), 3.54 (dd, 1H, J = 11.3 and 2.2 Hz); ^{13}C NMR (125 MHz, $CDCl_3$): δ 163.3, 158.8, 158.7, 150.9, 144.2, 139.5, 139.3 (q, J = 39.6 Hz), 135.2, 135.0, 130.15, 130.06, 128.10, 128.07, 127.2, 124.5, 120.2 (q, J = 268 Hz), 113.4, 102.5, 88.1, 87.2, 83.0, 81.6, 77.7, 68.05, 60.7, 55.3; ^{19}F NMR (470 MHz, CD_3CN): δ −63.51; HRMS (ESI-TOF) m/z: [M − H]$^-$ calcd for $C_{34}H_{31}F_3N_5O_8$ 694.2125, found 694.2119.

*3′-O-[(2-Cyanoethoxy)-(N,N-diisopropylamino)phosphinyl]-5′-O-(4,4′-dimethoxytrityl)-2′-O-[(4-trifluoromethyl-1H-1,2,3-triazol-1-yl)methyl]uridine (**10**).* Compound **9** (0.24 g, 0.35 mmol) was dried over P_2O_5 in a vacuum desiccator and dissolved in dry dichloromethane (2.0 mL). Triethylamine (244 μL, 1.75 mmol) and 2-cyanoethyl *N,N*-diisopropylphosphoramidochloridite (0.18 mL, 0.80 mmol) were added, and the mixture was stirred under nitrogen for 2 h. The reaction mixture was eluted through a short dried silica gel column (50−100% EtOAc and 5% Et_3N in hexane) to yield 0.33 g of **10** as white foam (87% yield, calculated by subtracting the mass of 2-cyanoethyl *N,N*-diisopropylphosphonamidate, the obtained side product according to the ^{1}H NMR spectrum). A 6:4 (*n*/*n*)-mixture of *Rp*/*Sp*-diastereomers was obtained (distinguished in the spectra as *I* (major diastereomer) and *II* (minor diastereomer)). ^{1}H NMR (500 MHz, CD_3CN): δ 8.52 (d, 0.6H, J = 0.7 Hz, *I*), 8.49 (d, 0.4H, J = 0.6 Hz, *II*), 7.86 (d, 0.4H, J = 8.2 Hz, *I*), 7.80 (d, 0.6H, J = 8.2 Hz, *II*), 7.49−7.45 (m, 2H), 7.38−7.27 (m, 7H), 6.93−6.90 (m, 4H), 6.15 (d, 0.4H, J = 11.5 Hz, *II*), 6.12 (d, 0.6H, J = 11.4 Hz, *I*), 6.06 (d, 0.6H, J = 11.4 Hz, *I*), 5.99 (d, 0.4H, J = 11.4, *II*), 5.91 (d, 0.4H, J = 2.2 Hz, *II*), 5.87 (d, 0.6H, J = 2.0 Hz, *I*), 5.17 (d, 0.4H, J = 8.2 Hz, *II*), 5.15 (d, 0.6H, J = 8.2, *I*), 4.62−4.53 (m, 1.4H), 4.46 (dd, 0.6H, J = 5.0 and 2.1 Hz, *I*), 4.23 (ddd, 0.4H, J = 7.4, 2.5, and 2.3 Hz, *II*), 4.17 (m, 0.6H), 3.86−3.82 and 3.74−3.59 (both m, 2H), 3.804 and 3.802 (both s, 0.4 × 6H, *II*), 3.797 (s, 0.6 × 6H, *I*), 3.57−3.48 (m, 3H), 3.45 (dd, 0.4H, J = 11.3 and 2.8 Hz, *II*), 3.41 (dd, 0.6H, J = 11.2 and 3.2 Hz, *I*), 2.70 (m, 0.6 × 2H), 2.55 (m, 0.4 × 2H), 1.15 (d, 0.4 × 6H, J = 6.7 Hz, *I*), 1.14 (d, J = 6.7 Hz, 0.6 × 6H, *II*), 1.08 (d, 0.4 × 6H, *II*), 1.05 (d, 0.6 × 6H, *I*); ^{13}C NMR (125 MHz, $CDCl_3$): δ 162.9 (both *I* and *II*), 158.83 and 158.82 (both *I* and *II*), 150.5 (*II*) 150.4 (*I*), 144.7 (*II*), 144.6 (*I*), 139.6 (*I*), 139.5 (*II*), 138.1 (q, J = 39.0 Hz, both *I* and II), 135.5 and 135.4 (*II*), 135.3 and 135.2 (*I*), 130.21, 130.18, 128.1, 128.0, and 127.1 (both *I* and *II*), 125.5 (m, *II*), 125.4 (m, *I*), 120.9 (q, J = 266.7 Hz, both *I* and *II*), 118.5 (*II*), 118.0 (*I*), 101.6 (*II*), 101.5 (*I*), 88.5 (*I*), 88.1 (*II*), 86.71 (*I*), 86.69 (*II*), 82.4 (d, J = 2.7 Hz, *II*), 81.8 (d, J = 6.4 Hz, *I*), 80.9 (*I*), 79.7 (d, J = 3.0 Hz, *II*), 78.1 (*I*), 77.7 (*II*), 69.6 (d, J = 14.0 Hz, *I*), 69.2 (d, J = 9.0 Hz, *II*), 60.99 (*I*), 60.93 (*II*), 58.2 (d, J = 7.3 Hz, *II*), 58.1 (d, J = 8.1 Hz, *I*), 54.97 and 54.94 (both *I* and *II*), 43.0

DOI: 10.1021/acs.joc.5b00973
J. Org. Chem. 2015, 80, 7961−7970

(d, J = 4.3 Hz, *II*), 42.9 (d, J = 4.5 Hz, *I*), 24.05, 23.98, 23.82, 23.76, 23.74, 23.68, 20.07, 20.02, and 19.97 (both *I* and *II*); ^{31}P NMR (200 MHz, CD_3CN): δ 150.5 and 150.8; ^{19}F NMR (470 MHz, CD_3CN): δ −61.52 and 61.60; HRMS (ESI-TOF) m/z: $[M + H]^+$ calcd for $C_{43}H_{50}F_3N_7O_9P$ 896.3360, found 896.3361.

*1-O-tert-Butyldimethylsilyl-3,4-O-isopropylidene-(2R,3R,4R)-6-methyl-2-[4-(trifluoromethyl)phenyl]hept-5-ene-1,2,3,4-tetraol (**12**).* 4-Bromobenzotrifluoride (3.4 g, 15 mmol) in dry diethyl ether (5 mL) was added slowly to a mixture of flakes of magnesium (0.37 g, 15 mmol) in dry diethyl ether (20 mL). The mixture was gently warmed up until it was spontaneously refluxed. The mixture was stirred for 1 h, and then, ketone **19**[33] (2.0 g, 6.1 mmol) in dry diethyl ether (10 mL) was slowly added. The reaction was stirred for 1 h at ambient temperature, acidified by aqueous HCl (1 mol L^{-1}) to pH 3.0, diluted with diethyl ether, and then, washed with brine. The organic layer was separated, dried with Na_2SO_4, filtered, and evaporated to dryness. The crude product was purified by silica gel chromatography (10% EtOAc in hexane) to give 2.1 g (73% yield) of **12** as a white foam (the undesired product with *S*-configured spiro carbon C-2 was obtained in 15% yield). ^{1}H NMR (500 MHz, $CDCl_3$): δ 7.70 (m, 2H), 7.56 (m, 2H), 4.96 (dd, 1H, J = 10 and 7.0 Hz), 4.60 (d, 1H, J = 7.0 Hz), 4.42 (m, 1H), 3.99 (d, 1H, J = 10.0 Hz), 3.55 (d, 1H, J = 10.0 Hz), 3.22 (s, 1H), 1.63 (b, 3H), 1.50 (s, 3H), 1.41 (s, 3H), 1.40 (b, 3H), 0.89 (s, 9H), 0.06 (s, 3H), 0.00 (s, 3H); ^{13}C NMR (125 MHz, CDCl3): δ 146.3, 135.2, 129.0 (q, J = 33 Hz), 126.8, 124.4 (q, J = 271 Hz), 124.0 (q, J = 2.5 Hz), 122.8, 108.0, 79.2, 75.0, 74.9, 68.9, 27.7, 25.9, 25.7, 25.2, 18.3, 17.8, −5.56, −5.57; ^{19}F NMR (470 MHz, $CDCl_3$): δ −64.34; HRMS (ESI-TOF) m/z: $[M + Na]^+$ calcd for $C_{24}H_{37}F_3NaO_4Si$ 497.2311, found 497.2334.

*1-O-Benzoyl-3,4-O-isopropylidene-(2R,3R,4R)-6-methyl-2-[4-(trifluoromethyl)phenyl]hept-5-ene-1,2,3,4-tetraol (**13**).* Compound **12** (2.0 g, 4.2 mmol) was dissolved in THF (30 mL), 1 mol L^{-1} TBAF in THF (5.0 mL, 5.0 mmol) was added, and the mixture was stirred overnight at ambient temperature. After completion of the reaction, $CaCO_3$ (1 g), strong cation-exchange resin (Dowex 50WX-200, 3 g), and methanol (3 mL) were added, and the mixture was stirred for 1 h and filtered through a Celite column. The filtrate was evaporated to dryness, evaporated with dry pyridine, and dissolved in dry pyridine (10 mL). A catalytic amount of DMAP and benzoyl chloride (0.54, 4.6 mmol) were added, and the mixture was stirred overnight at ambient temperature and extracted between saturated $NaHCO_3$ and dichloromethane. The organic layer was separated, dried with Na_2SO_4, filtered, and evaporated to dryness. The crude product was purified by silica gel chromatography (30% EtOAc in hexane) to give 1.9 g (98% yield) of **13** a white foam. ^{1}H NMR (500 MHz, $CDCl_3$): δ 7.90 (m, 2H), 7.77 (m, 2H), 7.63 (m, 2H), 7.60 (m, 1H), 7.43 (m, 2H), 5.03 (dd, 1H, J = 9.7 Hz and 6.7 Hz), 4.92 (m, 1H), 4.71−4.66 (m, 3H), 3.20 (s, 1H), 1.63 (s, 3H), 1.61 (s, 3H), 1.55 (s, 3H), 1.42 (s, 3H); ^{13}C NMR (125 MHz, $CDCl_3$): δ 166.6, 145.6, 137.4, 133.4, 129.6, 129.5 (m), 128.5, 126.9, 124.6 (q, J = 3.6 Hz), 124.2 (q, J = 270 Hz), 121.6, 108.3, 80.2, 75.9, 74.4, 69.3, 27.3, 25.9, 24.8, 18.0; ^{19}F NMR (470 MHz, $CDCl_3$): δ −62.50; HRMS (ESI-TOF) m/z: $[M + Na]^+$ calcd for $C_{25}H_{27}F_3NaO_5$ 487.1708, found 487.1748.

*5-O-Benzoyl-4-C-(4-trifluorophenyl)-2,3-O-isopropylidene-D-ribose (**14**).* A solution of osmium tetroxide (2.5 wt % in 2-methyl-2-propanol, 2.5 mL, 0.25 mmol) was added portion wise to a mixture of **13** (2.0 g, 4.2 mmol) and 4-methylmorpholine *N*-oxide (1.4 g, 12 mmol) in acetone (50 mL). The mixture was stirred overnight at ambient temperature and extracted between saturated $Na_2S_2O_5$ and ethyl acetate. The organic layer was separated, dried with Na_2SO_4, filtered, and evaporated to dryness. The residue (the vicinal diol intermediate) was dissolved in THF (25 mL), and H_5IO_6 (0.96 g, 4.2 mmol) was added. The mixture was stirred for 1 h at ambient temperature, concentrated, and purified by silica gel chromatography (30% EtOAc in hexane) to give 1.7 g (92% yield) of **14** as a colorless oil. ^{1}H NMR (500 MHz, $CDCl_3$): δ 7.87 (m, 2H), 7.64−7.59 (m, 5H), 7.54 (m, 1H), 7.39 (m, 2H), 5.69 (d, 1H, J = 3.0 Hz), 5.02 (d, 1H, J = 5.8 Hz), 4.89 (d, 1H, J = 11.7 Hz), 4.87 (d, 1H, J = 5.8 Hz), 4.59 (d, H, J = 11.7 Hz), 3.77 (d, 1H, J = 3.0 Hz), 1.27 (s, 3H), 1.02 (s, 3H); ^{13}C NMR (125 MHz, $CDCl_3$): δ 166.6, 142.8, 133.4, 129.7, 129.5 (m), 128.5, 127.1, 124.6 (q, J = 3.6 Hz), 124.2 (q, J = 270 Hz), 113.2, 102.3, 90.6, 86.7, 83.0, 69.7, 25.8, 25.7; ^{19}F NMR (470 MHz, $CDCl_3$): δ −64.38; HRMS (ESI-TOF) m/z: $[M + Na]^+$ calcd for $C_{22}H_{21}F_3NaO_6$ 461.1188, found 461.1176.

*1,2,3,5-Tetra-O-benzoyl-4-C-(4-trifluorophenyl)-D-ribose (**15**).* Compound **14** (1.6 g, 3.6 mmol) was dissolved in dioxane (80 mL), and 1.0 mol L^{-1} aq HCl (15 mL) was added. The mixture was stirred overnight at 55 °C, neutralized by addition of pyridine, and evaporated to dryness. The residue was evaporated with dry pyridine and dissolved in the same solvent. A catalytic amount of DMAP and benzoyl chloride (2.0 mL, 17 mmol) were added at 0 °C, and the mixture was allowed to warm up, stirred for 3 h at ambient temperature, quenched by methanol, and extracted between saturated $NaHCO_3$ and ethyl acetate. The organic layers were combined, dried with Na_2SO_4, filtered, and evaporated to dryness. The crude product was purified by silica gel chromatography (20% EtOAc in hexane) to give 2.1 g (81% yield) of **15** as a white foam (α/β = 1:4, n/n). ^{1}H NMR (500 MHz, $CDCl_3$): δ 8.22−7.20 (m, 24H), 7.16 (d, 0.2H, J = 4.6 Hz, α), 6.94 (s, 0.8H, β-anomer), 6.50 (d, 0.2H, J = 5.7 Hz, α-anomer), 6.47 (d, 0.8H, J = 5.0 Hz, β-anomer), 6.22 (dd, 0.2H, J = 5.7 and 4.8 Hz, α-anomer), 6.13 (d, 0.8H, J = 5.0 Hz, β-anomer), 4.87 and 4.78 (2 × d, 2 × 0.8H, J = 12.3 Hz both, β-anomer), 4.80 and 4.71 (2 × d, 2 × 0.2H, J = 12.1 Hz both, α-anomer); ^{13}C NMR (125 MHz, $CDCl_3$) for β-anomer only: δ 165.8, 165.1, 164.9, 164.8, 133.8, 133.73, 133.69, 133.3, 141.8, 130.5 (m), 130.1, 129.73, 129.65, 129.64, 129.5, 129.3, 128.87, 128.82, 128.58, 128.56, 128.4, 128.3, 127.2, 126.1 (q, J = 261 Hz), 125.0, 98.4, 87.6, 75.3, 72.2, 67.4; ^{19}F NMR (470 MHz, $CDCl_3$): δ −64.25 (β), −64.47 (α); HRMS (ESI-TOF) m/z: $[M + Na]^+$ calcd for $C_{40}H_{29}F_3NaO_9$ 733.1661, found 733.1691.

*2′,3′,5′-Tri-O-benzoyl-4′-C-(4-trifluoromethylphenyl)uridine (**16**).* Trimethylsilyltriflate (0.5 mL, 2.8 mmol) was added in drops to a mixture of 2,4-bis(trimethylsilyloxy)pyrimidine (0.55 g, 2.1 mmol) and **15** (0.26 g, 0.36 mmol) in dry acetonitrile (4 mL) under nitrogen (0 °C). The mixture was allowed to warm up, stirred overnight at room temperature, poured into cold saturated $NaHCO_3$, and extracted with chloroform. The combined organic layers were dried with Na_2SO_4, filtered, and evaporated to dryness. The residue was purified by silica gel chromatography (30% EtOAc in hexane) to give 0.18 g (72%) of **16** as a white foam. ^{1}H NMR (500 MHz, $CDCl_3$): δ 9.21 (b, 1H), 8.13 (d, 1H, J = 7.3 Hz), 7.69 (m, 4H), 7.63−7.46 (m, 10H), 7.27−7.23 (m, 4H), 6.61 (d, 1H, J = 6.0 Hz), 6.45 (d, 1H, J = 5.5 Hz), 6.08 (dd, 1H, J = 6.0 and 5.5 Hz), 5.57 (dd, 1H, J = 8.0 and 1.5 Hz), 4.85 (d, 1H, J = 12.5 Hz), 4.76 (d, 1H, J = 12.5 Hz); ^{13}C NMR (125 MHz, CDCl3): δ 165.8, 164.9, 164.8, 162.6, 150.3, 140.8, 139.0, 134.0, 133.9, 133.8, 130.8 (q, J = 33 Hz), 129.8, 129.7, 129.5, 129.0, 128.9, 128.5, 128.4, 128.2, 128.1, 126.4, 125.6 (q, J = 3.6 Hz), 123.8 (q, J = 270 Hz), 103.7, 87.5, 86.3, 73.4, 72.3, 68.3; ^{19}F NMR (470 MHz, CD_3CN): δ −64.75; HRMS (ESI-TOF) m/z: $[M + Na]^+$ calcd for $C_{37}H_{27}F_3KN_2O_9$ 739.1306, found 739.1311.

*5′-O-(4,4′-Dimetoxytrityl)-4′-C-(4-trifluoromethylphenyl)uridine (**18**).* Compound **16** (0.49 g, 0.70 mmol) was dissolved in a solution of 0.05 mol L^{-1} NaOMe in MeOH (10 mL). The mixture was stirred for 3 h at ambient temperature, neutralized by strong cation-exchange resin, and evaporated to dryness. The residue (**17**) was washed with hexane, evaporated with dry pyridine, and dissolved in a mixture of dichloromethane and pyridine (1:1, v/v, 5 mL). 4,4′-Dimethoxytrityl chloride (0.26 g, 0.77 mmol) was slowly added, and the mixture was stirred overnight at ambient temperature. The reaction was quenched by methanol, and the mixture was extracted between dichloromethane and saturated $NaHCO_3$. The organic layer was separated, dried with Na_2SO_4, filtered, and evaporated to dryness. The residue was purified by silica gel chromatography to give 0.51 g (40%) of **18** as a white foam. ^{1}H NMR (500 MHz, MeOD): δ 8.00 (d, 1H, J = 8.0 Hz), 7.54 (d, 2H, J = 8.5 Hz), 7.49 (d, 2H, J = 8.5 Hz), 7.35−7.22 (m, 9H), 6.84 (m, 4H), 6.17 (d, 1H, J = 4.5 Hz), 5.30 (d, 1H, J = 8.0 Hz), 4.76 (d, 1H, J = 5.0 Hz), 4.50 (dd, 1H, J = 5.0 and 4.5 Hz), 3.78 and 3.77 (2s, 2 × 3H), 3.60 (d, 1H, J = 11.0 Hz) and 3.37 (d, 1H, J = 11.0 Hz); ^{13}C NMR (125 MHz, CDCl3): δ 163.6, 158.8, 151.4, 144.0, 142.7, 140.4, 134.9, 134.7, 130.2, 130.1, 129.6 (q, J = 33 Hz), 128.1, 128.1, 127.3, 126.8, 124.8 (b), 124.1 (q, J = 270 Hz), 113.4, 113.3, 102.5, 90.2, 89.5,

DOI: 10.1021/acs.joc.5b00973
J. Org. Chem. 2015, 80, 7961−7970

87.6, 75.8, 72.4, 68.5, and 55.2; ^{19}F NMR (470 MHz, $CDCl_3$): δ −64.11; HRMS (ESI-TOF) m/z: $[M + Na]^+$ calcd for $C_{37}H_{33}F_3N_2NaO_8$ 713.2087, found 713.2089.

*5′-O-(4,4′-Dimetoxytrityl)-4′-C-(4-trifluoromethylphenyl)-2′-O-(triisopropylsilyloxymethyl)-uridine (**19**).* A mixture of **18** (0.11 g, 0.16 mmol), DIEA (68 μL, 0.40 mmol), and Bu_2SnCl_2 (56 mg, 0.17 mmol) in 1,2-dichloroethane (2 mL) was stirred for 1 h at ambient temperature. The mixture was then warmed up to 80 °C, and triisopropylsilyloxymethyl chloride (TOMCl, 52 μL, 0.21 mmol) was added over 90 min. The completed reaction mixture was diluted with dichloromethane, washed with saturated $NaHCO_3$, dried over Na_2SO_4, filtered, and evaporated to dryness. The residue was purified by silica gel chromatography (30% EtOAc in hexane) to give 67 mg (47%) of **19** as a white foam. ^{1}H NMR (500 MHz, CD_3CN): δ 7.67−7.65 (m, 3H), 7.54 (d, 2H, J = 8.3 Hz), 7.38−7.24 (m, 9H), 6.89−6.86 (m, 4H), 6.19 (d, 1H, J = 6.1 Hz), 5.49 (d, 1H, J = 8.2 Hz), 4.96 (s, 2H), 4.66 (d, 1H, J = 4.9 Hz), 4.58 (dd, 1H, J = 6.1 and 4.9 Hz), 3.783 and 3.779 (2*s*, 2 × 3H), 3.56 (d, 1H, J = 10.6 Hz), 3.34 (d, 1H, J = 10.6 Hz), 1.10−1.00 (m, 21H); ^{13}C NMR (125 MHz, CD_3CN): δ 162.8, 158.8, 144.4, 144.0, 140.3, 135.2, 135.1, 130.08, 130.06, 128.6 (q, J = 32 Hz), 128.02, 127.98, 127.2, 127.1, 124.5 (q, J = 270 Hz), 124.5 (b), 113.2, 102.4, 89.8, 89.5, 87.2, 86.7, 80.6, 71.6, 69.1, 60.0, 54.9, 17.2, and 11.7; ^{19}F NMR (470 MHz, CD_3CN): δ −64.59; HRMS (ESI-TOF) m/z: $[M + Na]^+$ calcd for $C_{47}H_{55}F_3N_2NaO_9Si$ 899.3527, found 899.3480.

*3′-O-[(2-Cyanoethoxy)-(N,N-diisopropylamino)phosphinyl]-5′-O-(4,4′-dimetoxytrityl)-4′-C-(4-trifluoromethylphenyl)-2′-O-(triisopropylsilyloxymethyl)uridine (**20**).* Compound **19** (50 mg, 57 μmol) was dried over P_2O_5 in a vacuum desiccator and dissolved in dry dichloromethane (0.3 mL). Triethylamine (55 μL, 0.4 mmol) and 2-cyanoethyl *N*,*N*-diisopropylphosphoramidochloridite (32 μL, 0.14 mmol) were added, and the mixture was stirred overnight at ambient temperature under nitrogen. The completed reaction mixture was eluted through a short silica gel column to yield 51 mg (83%) of the product (**20**) as a white foam (a mixture of diastereomers *I*(major)/*II*(minor): 7:3, *n*/*n*). ^{1}H NMR (500 MHz, CD_3CN): δ 7.71 (d, 0.7H, J = 8.2 Hz, *I*), 7.68−7.56 (m, 4.3H), 7.41−7.24 (m, 9H), 6.9−6.85 (m, 4H), 6.23 (d, 0.7H, J = 4.1 Hz), 6.17 (d, 0.3 H, J = 7.6 Hz), 5.55 (d, 0.3H, J = 8.1 Hz), 5.43 (d, 0.7H, J = 8.1 Hz), 4.95 and 4.93 (2 × d, 2 × 0.3H, J = 8.3 Hz both, *II*), 4.92 and 4.91 (2 × d, 2 × 0.7H, J = 8.9 Hz both, *I*), 4.82 (dd, 0.7H, J = 10.3 and 5.3 Hz, *I*), 4.71 (dd, 0.3H, J = 7.5 and 4.6 Hz, *II*), 4.58 (dd, 0.3H, J = 12.4 and 4.5 Hz, *II*), 4.54 (dd, 0.7H, J = 4.8 and 4.6 Hz, *I*), 3.87−3.67 (m, 2H), 3.793, 3.786, and 3.781 (each s, 6H), 3.66 and 3.47 (2 × d, 2 × 0.3H, J = 10.8 Hz, both, *II*), 3.59 and 3.44 (2 × d, 2 × 0.7H, J = 10.8 Hz both, *I*), 3.59−3.53 and 3.02−2.97 (m, 2H), 2.74−2.59 (m, 2H), 1.12−0.85 (m, 33H); ^{13}C NMR (125 MHz, CD_3CN): δ 162.9 (*I*), 162.7 (*II*), 158.82 (*II*), 158.79 (*I*), 150.6 (*II*), 150.4 (*I*), 144.5 (*I*), 144.4 (*II*), 144.1 (*I*), 144.0 (*II*), 141.0 (*I*), 140.2 (*II*), 135.2 (*I*), 135.1 (*II*), 130.2, 130.14, 130.08, 128.7 (q, J = 32.1 Hz, *I*), 128.5 (q, J = 31.9 Hz, *II*), 128.12, 128.08, 128.0, 127.6 (*II*), 127.4 (*I*), 127.1 (*II*), 127.0 (*I*), 124.6 (q, J = 271 Hz, *II*), 124.5 (q, J = 271 Hz, *I*), 124.4 (m), 118.8 (*II*), 118.6 (*I*), 113.28 and 113.26 (*II*), 113.16 and 113.14 (*I*), 102.7 (*II*), 102.2 (*I*), 89.8 (*I*), 89.8 (*I*), 89.2 (d, J = 10.1 Hz, *II*), 88.7 (*I*), 88.4 (d, J = 5.9 Hz, *I*), 87.4 (*II*), 86.8 (*I*), 85.6 (*II*), 79.0 (*I*), 77.8 (*II*), 73.6 (d, J = 7.0 Hz, *II*), 73.4 (d, J = 11.1 Hz, *I*), 69.07 (*II*), 67.7 (*I*), 58.2 (d, J = 20.8 Hz, *I*), 57.7 (d, J = 22.0 Hz, *II*), 54.96 (*II*), 5492 (*I*), 43.0 (d, J = 12.7 Hz, *I*), 42.7 (d, J = 12.2 Hz, *II*), 23.95, 23.87, 23.84, 23.78, 23.65, 23.60, 20.08, 20.02, 19.95, 17.23, 17.21, 11.73, and 11.70; ^{31}P NMR (200 MHz, CD_3CN): δ 151.18 (*II*) and 149.96 (*I*); ^{19}F NMR (470 MHz, CD_3CN): δ −64.57 (*II*) and −64.62 (*I*); HRMS (ESI-TOF) m/z: $[M + H]^+$ calcd for $C_{56}H_{73}F_3N_4O_{10}PSi$ 1077.4786, found 1077.4742.

Oligonucleotide Synthesis. Oligoribonucleotides **ORN 1−5** were synthesized in 1.0 μmol scale using an automatic DNA/RNA synthesizer. Benzylthiotetrazol was used as an activator. 0.11 mol L^{-1} solutions of **1** and **2** were used to load the synthesizer vessels. A coupling time of 300 s was used for the standard 2′-*O*-TBDMS- and 2′-*O*-Me RNA building blocks, and 600 s was used for **1** and **2**. According to the DMTr assay, the coupling efficiencies (>95%) of **1** and **2** was equal with those of the standard building blocks. Manual coupling was required for the coupling of **3**: A 0.20 mol L^{-1} solution of **3** (50 μL, 10 μmol) was mixed with a solution of benzylthiotetrazol (0.25 mol L^{-1} in dry acetonitrile, 40 μL, 10 μmol) and suspended with the CPG support (bearing the sequence before **3**, 1 μmol). The suspension was mixed for 10 min under nitrogen at ambient temperature, loaded onto the synthesis column, and filtered. The coupling was repeated, and the synthesis column was set to the synthesizer. The automatic chain elongation was then continued. According to the DMTr assay, **3** could be coupled in 90% yield. After the chain elongation, the oligonucleotides were released from the supports (in columns) by a mixture of concentrated ammonia and ethanol (3:1, v/v) for 3 h at 55 °C. The supports were removed by filtration, and the deprotection was then continued in the same mixture overnight at room temperature. The mixtures were evaporated to dryness, and the residues were dissolved in a mixture of triethylamine trihydrofluoride (75 μL), triethylamine (60 μL), and DMSO (115 μL) (for 2.5 h at 65 °C). NaOAc (0.1 mol L^{-1}, 10 mL) was added to each mixture, and loading onto an RP cartridge was carried out. Aqueous $Et_3N^+AcO^-$ (0.1 mol L^{-1}, 6.0 mL, pH = 7.0) was eluted though the cartridges, the crude RNAs were released by elution with 60% aqueous acetonitrile, and the RNA fractions were evaporated to dryness. The crude RNAs were dissolved in sterilized water, and then RP-HPLC was carried out. After RP-HPLC purification (a semipreparative RP-HPLC column (C-18, 250 mm × 10 mm, 5 μm) with a gradient elution of 0−90% acetonitrile in 0.1 mol L^{-1} triethylammonium acetate over 25 min, with detection at 260 nm), the homogenized RNAs were lyophilized, and their authenticity was verified by ESI-TOF MS (Table 1). Isolated yields (Table 1) for **ORN 1** (7%), **ORN 2** (10%), **ORN 3** (5%), **ORN 4** (7%), and **ORN 5** (7%) were determined from the UV absorbance at λ = 260 nm.

^{19}F NMR Spectroscopy Studies. The samples for the ^{19}F NMR measurements were prepared as we previously reported.[20] Similarly, the ^{19}F NMR parameters were the same: **ORN 1**, **ORN 2**, **ORN 3**, **ORN 4**, or **ORN 5** (25 nmol, as triethylammonium salts) was dissolved in a mixture of 10 mmol L^{-1} sodium cacodylate and 0.1 mol L^{-1} NaCl in D_2O/H_2O (1:9 v/v), pH = 6.0 or 7.0. All samples were heated to 90 °C and allowed to cool down to room temperature, and then, the NMR measurements were carried out at the target temperatures. Spectra were recorded at a frequency of 470.6 MHz. Typical experimental parameters were chosen as follows: ^{19}F excitation pulse, 4.0 μs; acquisition time, 1.17 s; prescan delay, 6.0 μs; relaxation delay, 0.8 s; and the usual number of scans was 2048 or 1024. The parameters were optimized to gain the signals with the longest relaxation rate. A macro command was used for automatic temperature ramps using a 20 min equilibration time for each temperature.

UV and CD Measurements. The melting curves (absorbance versus temperature) were measured at 260 nm on a UV−visible spectrometer equipped with a multiple cell holder and a Peltier temperature controller. The temperature was changed at a rate of 0.5 °C min^{-1} (between 10 and 90 °C). The measurements were performed in 10 mmol L^{-1} sodium cacodylate (pH 6.0 or 7.0). **ORN 1−5** were used at a concentration of 2 μmol L^{-1}. T_m values (Table 2) were determined as the maximum of the first derivate of the melting curve.

The CD spectra were measured using the same mixtures as used to obtain the UV-melting profiles. The sample temperature was changed at a rate of 0.5 °C min^{-1} (see the Supporting Information).

■ ASSOCIATED CONTENT

Supporting Information

NMR spectra for **9**, **10**, and **12−20**; RP-HPLC profiles and MS (ESI-TOF) spectra for **ORN 1−5**; UV-melting profiles of **ORN 4** and **ORN 5** + A_9 with and without neomycin; CD profiles of **ORN 1**, **ORN 4** and **ORN 5** + A_9; ^{1}H NMR data to determine the sugar puckering of **1**; and further ^{19}F NMR data for concentration-dependent triplex formation of **ORN 5**. The Supporting Information is available free of charge on the ACS Publications website at DOI: 10.1021/acs.joc.5b00973.

DOI: 10.1021/acs.joc.5b00973
J. Org. Chem. 2015, 80, 7961−7970

AUTHOR INFORMATION

Corresponding Author

*E-mail: pamavi@utu.fi.

Notes

The authors declare no competing financial interest.

ACKNOWLEDGMENTS

The financial support from the Academy of Finland (nos. 251539 and 256214) are gratefully acknowledged. We also thank Dr. Anu Kiviniemi for preliminary synthetic work of sensor **3**.

REFERENCES

(1) Hammann, C.; Norman, D. G.; Lilley, D. M. *Proc. Natl. Acad. Sci. U. S. A.* **2001**, *98*, 5503.
(2) Olsen, G. L.; Edwards, T. E.; Deka, P.; Varani, G.; Sigurdsson, S. Th.; Drobny, G. P. *Nucleic Acids Res.* **2005**, *33*, 3447.
(3) Kreutz, C.; Kählig, H.; Konrat, R.; Micura, R. *J. Am. Chem. Soc.* **2005**, *127*, 11558.
(4) Kreutz, C.; Kählig, H.; Konrat, R.; Micura, R. *Angew. Chem., Int. Ed.* **2006**, *45*, 3450.
(5) Hennig, M.; Munzarová, M. L.; Bermel, W.; Scott, L. G.; Sklenář, V.; Williamson, J. R. *J. Am. Chem. Soc.* **2006**, *128*, 5851.
(6) Graber, D.; Moroder, H.; Micura, R. *J. Am. Chem. Soc.* **2008**, *130*, 17230.
(7) Barhate, N. B.; Barhate, R. N.; Cekan, P.; Drobny, G.; Sigurdsson, S. Th. *Org. Lett.* **2008**, *10*, 2745.
(8) Hennig, M.; Scott, L. G.; Sperling, E.; Bermel, W.; Williamson, J. R. *J. Am. Chem. Soc.* **2007**, *129*, 14911.
(9) Kiviniemi, A.; Virta, P. *J. Am. Chem. Soc.* **2010**, *132*, 8560.
(10) Tanabe, K.; Sugiura, M.; Nishimoto, S. *Bioorg. Med. Chem.* **2010**, *18*, 6690.
(11) Moumné, R.; Pasco, M.; Prost, E.; Lecourt, T.; Micouin, L.; Tisne, C. *J. Am. Chem. Soc.* **2010**, *132*, 13111.
(12) Kiviniemi, A.; Virta, P. *Bioconjugate Chem.* **2011**, *22*, 1559.
(13) Sakamoto, T.; Hayakawa, H.; Fujimoto, K. *Chem. Lett.* **2011**, *40*, 720.
(14) Sakamoto, T.; Shimizu, Y.; Sasaki, J.; Hayakawa, H.; Fujimoto, K. *Bioorg. Med. Chem. Lett.* **2011**, *21*, 303.
(15) Lombés, T.; Moumné, R.; Larue, V.; Prost, E.; Catala, M.; Lecourt, T.; Dardel, F.; Micouin, L.; Tisné, C. *Angew. Chem., Int. Ed.* **2012**, *51*, 9530.
(16) Fauster, K.; Kreutz, C.; Micura, R. *Angew. Chem., Int. Ed.* **2012**, *51*, 13080.
(17) Riedl, J.; Pohl, R.; Rulíšek, L.; Hocek, M. *J. Org. Chem.* **2012**, *77*, 1026−1044.
(18) Kiviniemi, A.; Murtola, M.; Ingman, P.; Virta, P. *J. Org. Chem.* **2013**, *78*, 5153.
(19) Tanabe, K.; Tsuda, T.; Ito, T.; Nishimoto, S. *Chem. - Eur. J.* **2013**, *19*, 15133.
(20) Granqvist, L.; Virta, P. *J. Org. Chem.* **2014**, *79*, 3529.
(21) Košutić, M.; Jud, L.; Da Veiga, C.; Frener, M.; Fauster, K.; Kreutz, C.; Ennifar, E.; Micura, R. *J. Am. Chem. Soc.* **2014**, *136*, 6656.
(22) Chen, H.; Viel, S.; Ziarelli, F.; Peng, L. *Chem. Soc. Rev.* **2013**, *42*, 7971.
(23) Gerig, J. T. In *Biological Magnetic Resonance*; Berliner, L., Reuben, J., Eds.; Plenum Press: New York, 1978; p 139.
(24) Rastinejad, F.; Evilia, C.; Lu, P. *Methods Enzymol* **1995**, *261*, 560.
(25) Gerig, J. T. *Prog. Nucl. Magn. Reson. Spectrosc.* **1994**, *26*, 293.
(26) Kitevski-LeBlanc, J. L.; Prosser, R. S. *Prog. Nucl. Magn. Reson. Spectrosc.* **2012**, *62*, 1.
(27) Lee, Y.; Zeng, H.; Ruedisser, S.; Gossert, A. D.; Hilty, C. *J. Am. Chem. Soc.* **2012**, *134*, 17448−17451.
(28) Meier, S.; Jensen, P.; Karlsson, M.; Lerche, M. *Sensors* **2014**, *14*, 1576.
(29) Zengeya, T.; Gupta, P.; Rozners, E. *Angew. Chem., Int. Ed.* **2012**, *51*, 12593−12596.
(30) Zavgorodny, S. G.; Pechenov, A. E.; Shvets, V. I.; Miroshnikov, A. I. *Nucleosides, Nucleotides Nucleic Acids* **2000**, *19*, 1977−1991.
(31) Efimov, V. A.; Aralov, A. V.; Fedunin, S. V.; Klykov, V. N.; Chakhmakhcheva, O. G. *Russ. J. Bioorg. Chem.* **2009**, *35*, 250−253.
(32) Stepanova, N. P.; Galishev, V. A.; Turbanova, E. S.; Maleev, A. V.; Potekhin, K. A.; Kurkutova, E. N.; Struchkov, Yu. T.; Petrov, A. A. *Zh. Org. Khim.* **1989**, *25*, 1613.
(33) Chen, B.; Jamieson, E. R.; Tullius, T. D. *Bioorg. Med. Chem. Lett.* **2002**, *12*, 3093.
(34) Orita, A.; Hamada, Y.; Nakano, T.; Toyoshima, S.; Otera. *Chem. - Eur. J.* **2001**, *7*, 3321.
(35) Davies, D. B. *Prog. Nucl. Magn. Reson. Spectrosc.* **1978**, *12*, 135.
(36) Hoyne, P. R.; Gacy, A. M.; McMurray, C. T.; Maher, L. J., III *Nucleic Acids Res.* **2000**, *28*, 770.
(37) Mitton-Fry, R. M.; DeGregorio, S. J.; Wang, J.; Steitz, T. A.; Steitz, J. A. *Science* **2010**, *330*, 1244−1247.
(38) Brown, J. A.; Valenstein, M. L.; Yario, T. A.; Tycowski, K. T.; Steitz, J. A. *Proc. Natl. Acad. Sci. U. S. A.* **2012**, *109*, 19202−19207.
(39) Arya, D. P. *Acc. Chem. Res.* **2011**, *44*, 134−146.

DOI: 10.1021/acs.joc.5b00973
J. Org. Chem. 2015, 80, 7961−7970